Semiconductor Physics, Quantum Electronics & Optoelectronics, 2006. V. 9, N 4. P. 21-25.

PACS 72.20.-i, 72.20.-r, 73.50.Pz, 73.61.Wp, 78.40.Ri, 78.66.Tr

Photoabsorption and photoconductivity in C_{60} layers

St. Kanev, Z. Nenova, N. Koprinarov
Central Laboratory of Solar Energy and New Energy Sources, Bulgarian Academy of Sciences
72, "Tzarigradsko chaussee" blvd, 01784 Sofia, Bulgaria
Phone: +3592778448, fax: +35928754016
E-mail: kanevstefan@yahoo.com, znenova@yahoo.com

Abstract. A complex investigation of the photoconductivity of fullerene films, prepared by thermal evaporation in vacuum, was carried out. The investigated films contain predominantly C_{60} in various phases as shown elsewhere. The multiple photocurrent spectra analysis (MPSA method) has been used in the current study. The MPSA method utilizes a family of routine photocurrent spectra, measured at various intensities generated by the light source. A suitable data processing of such a family allowed several basic characteristics of the films to be obtained – the optical bandgap, subbandgap optical absorption spectra, features of shallow and deep defect states as well as the spectra of the power index in the dependence of the photocurrent on the photon flux. These characteristics were interpreted in terms of structural features of the investigated samples. Conclusions about applications of such C_{60} films were made.

Keywords: photoconductivity, C_{60} fullerene, optical absorption.

Manuscript received 11.09.06; accepted for publication 23.10.06.

1. Introduction

In more than a decade, a variety of thin film materials has been studied as potential candidates for application in low-cost photovoltaic solar cells. Regardless of the intensive research in the field, a universal favorite, satisfying technological and quality demands, is not established yet. The fullerene films (C_{60}) could be considered as attractive for photovoltaic solar energy conversion due to the high photoconductivity of the material and because of the favorable bandgap width that can be tailored in the range of 1.6 to 2.3 eV [1-6]. New, simple and productive preparation methods for C_{60} are already developed. They provide opportunity for low cost roll-to-roll production of flexible solar cells on large area cheap substrates. Other applications of C_{60}, such as in thin-film photoelectric devices [7, 8], gas sensors, electrochromic material [9], doping impurity for conductive polymer films, superconductors [9] and for information storage [10] are of interest, too [11-13]. Thus, detailed investigations of the photoelectric behavior of C_{60} and its stability under various ambient conditions are of significant interest.

2. Experimental details

The samples for this study were deposited by using direct vacuum sublimation from fullerene containing carbon soot without intermittent enrichment or separation of the fullerene fractions. This method was chosen because of its simplicity and low production cost. The evaporation temperature was kept at 550 ºC, which results in predominantly C_{60} containing deposits on glass substrates at room temperature. Samples of the thickness between 0.3 and 1.2 μm were prepared. A more detailed study of the film content and structure is presented in [14], where it was revealed that the films consist of microcrystallites, uniformly dispersed in an amorphous matrix. Coplanar aluminium ohmic contacts, separated by a 0.8 mm gap, were evaporated onto the films for the conductivity measurements.

A standard set-up was used for the measurements of the photocurrent spectra, including a light source generating variable light intensities (W-halogen lamp with a variable power supply), a monochromator and a sample compartment attached to an electrometer, connected by a computerized data acquisition block, a

spectrally nonselective radiometer checked the light intensity at the monochromator outlet.

To avoid humidity effects [14] the presented measurements were carried out at 30 % ambient humidity. The photocurrent at each measurement point was recorded after reaching a steady state value (about 30 s after any change of illumination conditions).

3. Measurement of the multiple photocurrent spectra

To perform a complex investigation of the photoelectric behavior of the available C_{60} films, we used the multiple photocurrent spectra analysis (MPSA) method. This method was proposed and described in more detail in our previous publication [15].

As a preliminary step to the measurements, the light source was calibrated at various intensities. A nonselective radiometer located at the sample holder was used for the purpose. A family of spectra was measured – each one obtained by a wavelength scan, performed at a certain voltage applied to the lamp. The whole family of spectra was established by applying various illumination intensities obtained by varying the voltage at the light source. The family of such baselines is shown in Fig. 1 in terms of photon flux reaching the surface of the sample versus wavelength and with the lamp voltage as a variable parameter.

The major experimental procedure of the MPSA method consists of measuring a number of photocurrent spectra of the investigated sample, carried out at several lamp voltages. Typically, voltages from the same set, applied to the lamp during the calibration, were used in this step, too. A family of such spectra (shortly referred to here as multiple photocurrent spectra (MPS)) is shown in Fig. 2. The presented MPS were obtained by measuring a typical 0.8 μm thick fullerene (C_{60}) sample. Further, the MPS and the lamp calibration spectra were used to derive several basic characteristics of the investigated sample.

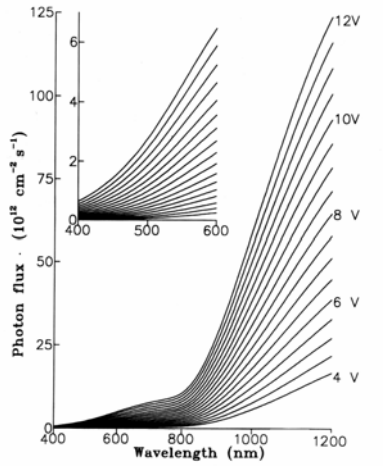

Fig. 1. A family of lamp calibration spectra. Each curve represents the photon flux, reaching the sample surface, versus the incident light wavelength for the indicated lamp voltage.

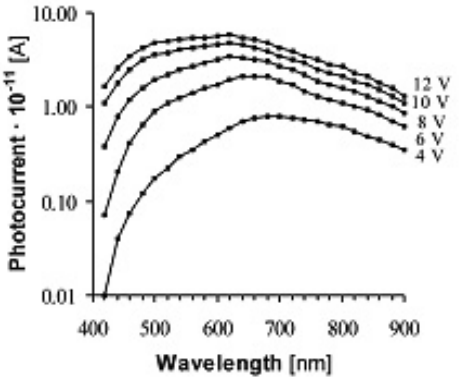

Fig. 2. Multiple photocurrent spectra of a 0.8 μm thick fullerene film. Each spectrum was obtained with the lamp voltage kept at the indicated value.

4. Results

Fig. 3 shows a family of dependences of the photocurrent (I_{ph}) on the incident photon flux (Φ) for various wavelengths (λ). Each curve is obtained by presenting the I_{ph} values, corresponding to the certain λ in MPS, as a function of the Φ values that match the equivalent lamp voltages at the same λ from the calibration data. Note that each curve in Fig. 3 is almost linear in the large range of Φ values as presented in double logarithmic scales. This indicates the power dependence between the photocurrent and the incident photon flux in this range:

$$I_{ph} = C \cdot \Phi^{\beta}. \qquad (1)$$

The power index β varies slightly with λ (change of the slope at various constant values of λ). As the power index in this dependence is related to the photo-carrier recombination processes, the reconstruction of its spectra shown in Fig. 7 is of interest too and will be discussed later.

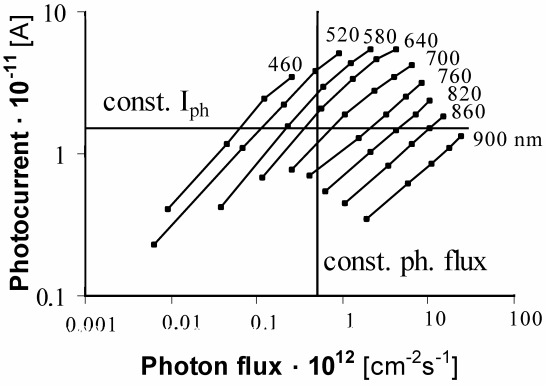

Fig. 3. Dependences between the photocurrent and the photon flux at various incident light wavelengths for the sample from Fig. 2. Each curve was obtained by processing the data from Figs 1 and 2 as explained in the text.

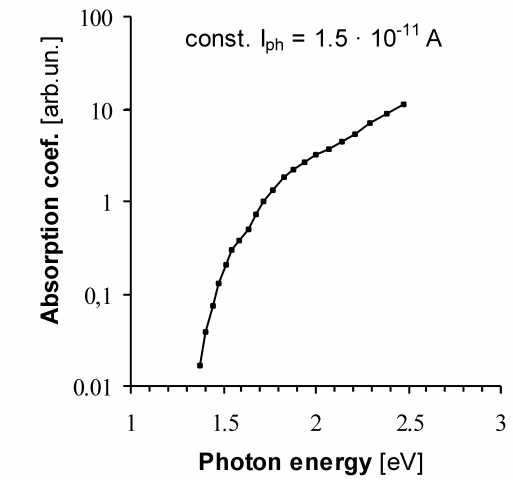

Fig. 4. Optical absorption spectrum of the fullerene sample in the region of weak absorption. The spectrum was obtained by processing the data from Fig. 3 where the constant photocurrent (I_{ph} = 1.5·10^{-11} A) is kept.

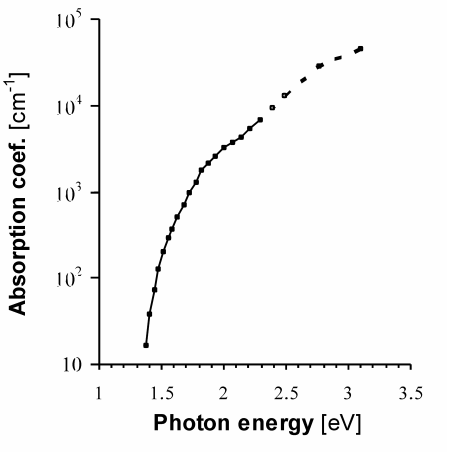

Fig. 5. Complete optical absorption spectrum of the investigated film as obtained by fitting the spectrum from Fig. 4 to the data from the photometric measurements.

The subbandgap optical absorption is an important characteristic of the investigated sample that contains information about the features of the defect states in the material. Usually, the constant photocurrent method (CPM) [16] is used for determination of this characteristic of photoconductive thin films. The essence of CPM is that the photocurrent in the sample is kept constant during the wavelength scan by varying (and measuring) the photon flux Φ_λ of the incident light. As shown by Vanecek *et al*. [16] the following simple relation is valid in these conditions in the low absorption region ($\alpha(\lambda)$<1):

$$\alpha(\lambda) = \text{const}/\Phi(\lambda), \qquad (2)$$

where $\alpha(\lambda)$ is the optical absorption coefficient and $\Phi(\lambda)$ is the incident photon flux at the same λ. One can note that the points, obtained by a cross-section of the family of $(I_{ph} - \Phi)_\lambda$ dependences in Fig. 3 at the certain I_{ph} level (I_c = const indicated by a horizontal line), fulfill the conditions of CPM. Thus, the subbandgap absorption spectra of the studied C_{60} films can be reconstructed by using the MPSA data as shown in Fig. 4. The data in this figure are presented in arbitrary units as follows from the undefined constant in Eq. (2). The complete optical absorption spectrum of the investigated film is shown in Fig. 5 in absolute units. As usual, this spectrum has been obtained by fitting of the weak absorption part from Fig. 4 to the strong one, obtained by photometric measurements (a double beam spectrophotometer "Perkin Elmer 330").

On the other hand, a cross-section of the data in Fig. 3 at the constant value of the photon flux (vertical line) can be used for obtaining the correct spectrum of sample photoconductivity without the need of any normalization procedure. These spectra at two different photon flux values are shown in Fig. 6.

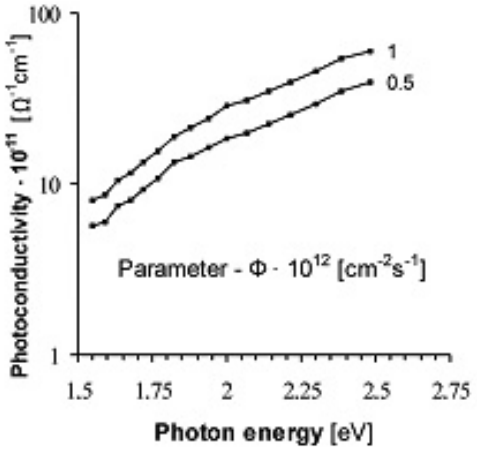

Fig. 6. Photoconductivity spectra of the investigated fullerene film at various constant photon fluxes. With the increase of Φ, the quantum efficiency decreases.

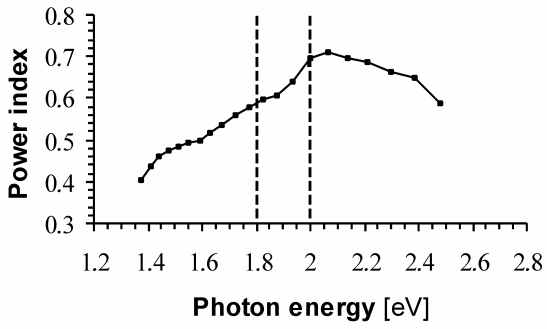

Fig. 7. Variation of the power index β (Eq. (1)) with the photon energy for the investigated fullerene film.

5. Discussion

The complete optical absorption spectrum (Fig. 5) of the investigated C_{60} film appears similar to that of other thin films of interest for application in solar cells (e.g. a-Si:H). However, several specific features can be observed. The optical gap of the fullerene films can be characterized by the value $E_{04} = 2.4$ eV (the photon energy at $\alpha = 10^4$ cm^{-1}). This value is higher than the corresponding values of other materials appropriate for active absorption layers in solar cells (e.g. a-Si:H with typical E_{04} of about 1.6–1.8 eV). On the other hand, the larger bandgap of C_{60} films makes them interesting for application as window layers in hybrid thin-film solar cells. The low absorption part is rather smooth and falls down to significantly low values at low energy. This indicates absence of discrete photoactive electron levels in the gap and relatively low density of deep defects. An interesting feature of subbandgap absorption is a small kink at 1.8-2.0 eV (690–617 nm) that can be observed in Figs 4-6. A simple exponential decay (Urbach tail), originating from shallow localized tail states, can be expected in this region. In contrast, two exponential decays (lines in semilog. scale) with different characteristic energies $\Delta E_1 = 155$ meV and $\Delta E_2 = 300$ meV can be distinguished. This feature can be explained by the presence of two phases in the investigated film [14]. The part with lower characteristic energy could be associated with the crystalline C_{60} fraction, while that with wider tail with an amorphous phase. Thus, one can assume that the photons with energy bellow 1.8 eV are absorbed predominantly by the crystalline fraction and those with energy above 2.0 eV by the amorphous one. This assumption is supported also by the change of the power index in the ($I_{ph} - \Phi$) dependence at 1.8-2.0 eV that can be clearly seen in Fig. 7. Such a change obviously originates from a change in the recombination mechanism of the photo-generated carriers.

Another interesting feature can be seen clearly from comparison of Figs 5 and 6. The photoconductivity spectra has monotonously rising up to an energy as high as 2.5 eV (Fig. 6). The value of α reaches more than $2 \cdot 10^4$ cm^{-1} at this energy, which corresponds to light penetration depth of about 0.5 μm – smaller than the film thickness. An influence of the surface recombination should be expected at such a strong absorption, which usually demonstrates in a sharp decrease of photoconductivity spectra. In contrast, the rise of photoconductivity continues in this region, indicating that the surface recombination of the investigated film is negligible compared to the bulk one. This could be related to the closed atomic structure of C_{60}.

5. Conclusion

In this work, we have shown that the MPSA method can be successfully applied for investigation of C_{60} films. Information about the optical bandgap, the subbandgap optical absorption, the features of the shallow and deep defect states as well as some peculiarities of the carrier generation-recombination processes in the investigated material can be obtained by using this method.

The availability of two phases in the C_{60} films prepared by direct vacuum sublimation from carbon soot has found. In support of the availability of the two phases are the kink in the subbandgap absorption spectra and the change of the power factor in the dependence of the photocurrent on the incident photon flux at around 1.8 and 2.0 eV. These two phases exhibit different effective optical gaps (1.8 eV for "c" phase and 2.0 eV for "a" phase). This can be used for tailoring the apparent optical gap of the film material by varying the relative amount of these two phases.

The investigated films have a large characteristic optical gap – typically $E_{04} = 2.2 \ldots 2.4$ eV. They also exhibit a negligible surface recombination. These electronic characteristics make them interesting candidates for application in tandem solar cells as well as window layers in hybrid thin-film solar cells.

Acknowledgements

The sponsorship of the Bulgarian Ministry for Science and Education under contract F-329 is appreciated.

References

1. T. Takahashi, S. Suzuki, T. Morikawa, H. Katayama-Yoshida, S. Hasegawa, H. Inokuchi, K. Seki, K. Kikuchi, S. Suzuki, I. Ikemoto, Y. Achiba, Pseudo-gap at the Fermi level in K_3C_{60} observed by photoemission and inverse photoemission // *Phys. Rev. Lett.* **68** (8), p.1232-1235 (1992).
2. S. Saito, A. Oshiyama, Cohesive mechanism and energy bands of solid C_{60} // *Phys. Rev. Lett.* **66**, p. 2637-2640 (1991).
3. J.H. Weaver, J.L. Martins, T. Komeda, Y. Chen, T.R. Ohno, G.H. Kroll, N. Troullier, R.E. Haufler, R.E. Smalley, Electronic structure of solid C_{60}: experiment and theory // *Phys. Rev. Lett.* **66** (13), p. 1741-1744 (1991).
4. A. Skumanich, Optical absorption spectra of carbon 60 thin films from 0.4 to 6.2 eV // *Chem. Phys. Lett.* **182** (5), p. 486-490 (1991).
5. H. Imahori, Y. Mori, Y. Matano, Nanostructured artificial photosynthesis // *J. Photochem. Photobiol.* C **4**, p. 51-83 (2003).
6. K. Pichler, S. Graham, O.M. Gelsen, R.H. Friend, W. J. Romanow, J.P. McCauley, N. Coustel, J.E. Fischer, A.B. Smith, Photophysical properties of solid films of fullerene, C_{60} // *J. Phys.: Condens. Matter.* **3** (47), p. 9259-9270 (1991).
7. H. Hoppe, N. Arnold, D. Meissner, N.S. Sariciftci, Modeling of optical absorption in conjugated

polymer/fullerene bulk-heterojunction plastic solar cells // *Thin Solid Films* **451-452**, p. 589-592 (2004).

8. I. Riedel, V. Dyakonov, Influence of electronic transport properties of polymer-fullerene blends on the performance of bulk heterojunction photovoltaic devices // *Phys. status solidi* (*a*) **201** (6), p. 1332-1341 (2004).
9. P.R. Somani, S. Radhakrishnon, Electrochromic materials and devices: present and future // *Mater. Chem. Phys*. **77**(1), p. 117-133 (2003).
10. S. Margadonna, K. Prassides, Recent advances in fullerene superconductivity // *J. Solid State Chem.* **168** (2), p. 639-652 (2002).
11. P. Byszewski, E. Kowalska, M. Popiawska, M. Juczak, Z. Klusek, Molecules for information storage // *J. Mag. Mag. Mat***. 249**, p. 486 (2002).
12. C.C. Wang, Z.X. Guo, S.K. Fu, W. Wu, D.B. Zhu, Polymers containing fullerene or carbon nanotube structures // *Progr. Polym. Sci.* **29**, p. 1079-1141 (2004).
13. W.N. Sisk, D.H. Kang, M.Y.A. Raja and F. Farahi, Photocurrent and optical limiting studies of C_{60} films and solutions // *Intern. J. Optoelectronics* **11**, p. 325 (1997).
14. St. Kanev, Z. Nenova, N. Koprinarov, K. Ivanova, Conductivity and photoconductivity peculiarities observed in C_{60} layers // *Semiconductor Physics, Quantum Electronics and Optoelectronics* **9**(4), p. 17-20 (2007).
15. St. Kanev, Z. Nenova, K. Ivanova, S. Koynov, Characterization of a-Si:H films via analysis of multiple photocurrent spectra // *Sol. Energy Mater. Sol. Cells* **36**, p. 277-287 (1995).
16. M. Vanecek, J. Kocka, J. Stuchlik, A. Triska, Direct measurement of the gap states and band tail absorption by constant photocurrent method in amorphous silicon // *Solid State Communs* **39**, (11), p. 1199-1202 (1981).